Research Report

Attentional shifts towards an expected visual target alter the level of alpha-band oscillatory activity in the human calcarine cortex

Noriko Yamagishi [a,*], Naokazu Goda [a], Daniel E. Callan [a],
Stephen J. Anderson [b], Mitsuo Kawato [a]

[a]ATR Computational Neuroscience Laboratories, 2-2-2 Hikaridai, Seika-cho, Soraku-gun, Kyoto 619-0288, Japan
[b]The Wellcome Trust Laboratory for MEG Studies, Neurosciences Research Institute, School of Life and Health Sciences, Aston University,
Birmingham B4 7ET, UK

Abstract

Neuronal operations associated with the top–down control process of shifting attention from one locus to another involve a network of cortical regions, and their influence is deemed fundamental to visual perception. However, the extent and nature of these operations within primary visual areas are unknown. In this paper, we used magnetoencephalography (MEG) in combination with magnetic resonance imaging (MRI) to determine whether, prior to the onset of a visual stimulus, neuronal activity within early visual cortex is affected by covert attentional shifts. Time/frequency analyses were used to identify the nature of this activity. Our results show that shifting attention towards an expected visual target results in a late-onset (600 ms postcue onset) depression of alpha activity which persists until the appearance of the target. Independent component analysis (ICA) and dipolar source modeling confirmed that the neuronal changes we observed originated from within the calcarine cortex. Our results further show that the amplitude changes in alpha activity were induced not evoked (i.e., not phase-locked to the cued attentional task). We argue that the decrease in alpha prior to the onset of the target may serve to prime the early visual cortex for incoming sensory information. We conclude that attentional shifts affect activity within the human calcarine cortex by altering the amplitude of spontaneous alpha rhythms and that subsequent modulation of visual input with attentional engagement follows as a consequence of these localized changes in oscillatory activity.
© 2005 Elsevier B.V. All rights reserved.

1. Introduction

The deployment of covert attention towards a given visual target facilitates the detection of that target [24]. It has been hypothesized that this effect results from an enhancement of neuronal (visual) responses to the attended target and/or a suppression of responses to non-attended targets [42,51,52]. The modulation of visual input is purported to reflect at least three neuronal operations: the disengagement, shifting and engagement of attention [39,42,43]. Within this context, it is useful to distinguish between the neural processes that may be associated with attentional modulation per se versus those associated with shifting attention from one location to another. Attentional shifts are generally considered to reflect top–down control processes, whereas the modulation of visual input with attentional engagement follows as a consequence of these processes [26]. Liu et al. [30] have recently used the terms 'transient' and 'sustained' to distinguish between the neural processes associated with attentional shifts and attentional modulation, respectively.

* Corresponding author. Fax: +81 774 95 1236.
  E-mail address: n.yamagishi@atr.jp (N. Yamagishi).

Converging evidence from functional neuroimaging studies on humans [10,20,26,29], physiological studies on macaque [8,21,22] and behavioral studies on brain-damaged patients [14] suggests that top–down attentional control processes encompass the superior frontal, inferior parietal and superior temporal cortex. It is accepted that the attentional modulation of activity observed within extrastriate visual areas is a direct consequence of these control processes [7,26,60]. Whether such top–down processes have a similar influence on the striate cortex or not has been a matter of debate for some time. Recent studies suggest that they do [18,44,52,53,63,66] and that attentional engagement modulates activity within early visual areas by altering the amplitude of alpha-band activity and other natural brain rhythms [66]. The nature of any neuronal changes in early visual areas resulting from top–down attentional control processes alone (i.e., prior to stimulus onset) is not known.

Because attentional control processes involve a distributed network of cortical areas [26], their neural basis may well encompass changes in oscillatory brain activity (see [4,56,62]). It is known, for example, that the level of alpha-band activity is dependent on the behavioral significance of stimuli and is related to the degree of stimulus expectancy [3,6,62] (for a general review on alpha activity, see [49]). Either evoked (phase-locked) or induced (non phase-locked) oscillatory activity may serve to alter behaviorally relevant cortical processes. Although hemodynamic measures cannot distinguish between evoked and induced activity, electromagnetic response measures can, and this is one reason why we chose MEG to investigate the effects of attentional processes on human vision. This technique has a spatial resolution approaching that of fMRI for shallow sources [50] and millisecond temporal resolution.

MEG was used in combination with magnetic resonance imaging (MRI) to determine whether, prior to the onset of a visual stimulus, neuronal activity within early visual areas is affected by covert attentional shifts. To achieve this, we used red/green-modulated gratings as our stimuli because they evoke strong responses from the human calcarine cortex [1,2,12,17,66], an area that is well resolved with MEG [25]. The changes in cortical activity associated with shifting attention towards the chromatic grating were compared with those associated with shifting attention away from the grating. This 'subtraction paradigm' was employed because attentional processes per se may be associated with a complex distribution of cortical sources [38,47,49], whereas our goal was to characterize those sources specific for the task of shifting attention to an expected visual stimulus. In order to distinguish the respective cue-related (control of attention) and stimulus-related (effect of attention) responses, the cue to shift attention either towards or away from the stimulus preceded its onset by either 500 ms or 1000 ms (Fig. 1). Independent component analysis (ICA) and dipolar source modeling were used to confirm that the recorded MEG signals to attentional shifts originated from within the calcarine, and time/frequency analyses were used to identify the nature of this activity.
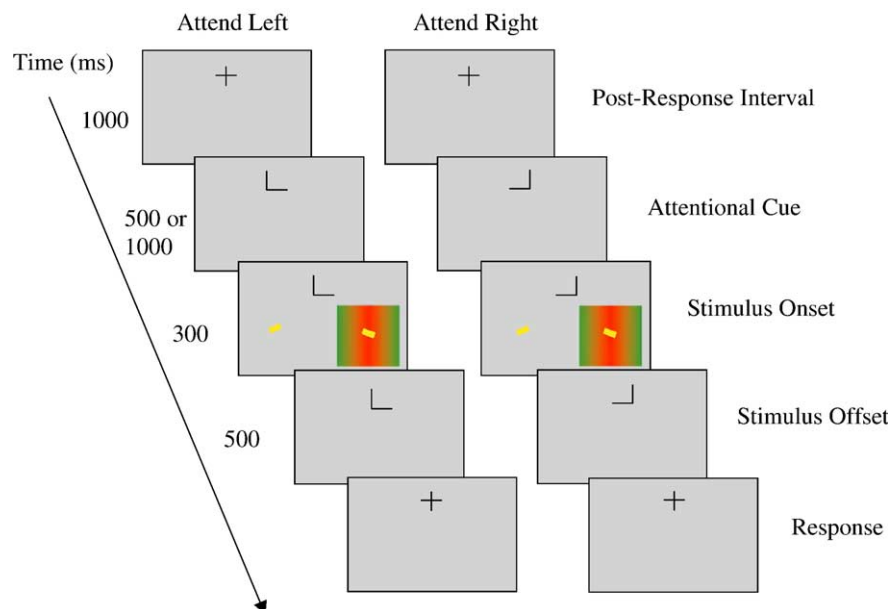

Fig. 1. Schematic illustration of a trial sequence. Observers covertly oriented their attention towards the right or left visual field as soon as the fixation mark changed from a cross to an L-shaped pattern. On each trial, the cue for directing attention to the right or left was selected at random with equal probability. After 500 ms or 1000 ms, the grating stimulus was presented (for 300 ms) in the lower right visual field. Coincident with the onset of the grating, a small yellow bar was presented (for 300 ms) in each quadrant of the inferior field. The L-shaped attentional cue reverted back to a cross 500 ms after the offset of the grating, which was the signal for each observer to record their judgment of the yellow bar's orientation on the side to which they had attended. Following this judgment, for which no response deadline was imposed, the central fixation cross remained for a further 1000 ms before the attentional cue was again presented.

2. Materials and methods

2.1. Stimuli

A chromatically modulated sinusoidal grating was generated using a VSG2/3 graphics board from Cambridge Research Systems (CRS, UK). To ensure the excitations of the long (L) and middle (M) wavelength-sensitive cones co-varied, the grating was modulated in color along the L−M cardinal direction of color space around an average white point (CIE coordinates $x = 0.31$, $y = 0.32$). The magnitude of the color modulations was set at 60% of the maximum available saturation of the display. The grating was stationary, oriented vertically, had a periodicity of 1 c/degree, subtended 9° square at a viewing distance of 170 cm and was physically equiluminant. Its absolute phase varied randomly from trial to trial. The grating was projected (ELP-710 projector, Epson, Japan) from outside a magnetically shielded room (Tokin Corp., Sendai, Japan) onto a semi-translucent screen inside the room and viewed against a white background. The mean luminance of the background and grating was the same, namely, 80 cd/m^2. The fixation target was a small black cross. The grating was confined to a single quadrant of the visual field (lower, right) to avoid signal cancellation between the upper and lower banks of the calcarine sulcus and simplify dipolar source analysis [27]. The upper and left-hand edges of the grating were positioned 1° from the horizontal and vertical meridian, respectively. Viewing was binocular, and the head was stabilized using a chin rest.

2.2. Procedure

The general procedure is depicted schematically in Fig. 1. Observers maintained central fixation throughout the entire experiment ($n = 400$ trials). There were two experimental conditions: in one condition, attention was shifted towards the stimulus ($n = 200$) and, in another condition, away from the stimulus ($n = 200$). The cue for shifting attention was a change in the fixation target from a cross to a small (0.5°) L-shaped pattern, which was oriented either rightwards or leftwards (see Fig. 1). The two conditions were presented in pseudo-random order, and the order of conditions varied across subjects. To help maximize attention, the grating was presented (for 300 ms) after an interstimulus interval (ISI) of either 500 ms ($n = 200$) or 1000 ms ($n = 200$). The two ISI conditions were presented in pseudo-random order. Because previous ERP studies showed that shifting attention-related activities occur at both early (~200 ms) and late (500–800 ms) latencies of the postcue period [23,37,67,68] and more recent studies suggesting only at late latencies [13,16,61,65], we treated trials containing an ISI of 1000 ms as the main condition with which to investigate the neural effects of attentional shifts.

Coincident with the onset of the grating, a small yellow bar (CIE coordinates: $x = 0.33$, $y = 0.36$; size: 0.4° vertically by 1° horizontally) was presented (for 300 ms) in each quadrant of the inferior visual field. The subject's task was to judge whether the bar at the attended location was clockwise or anti-clockwise oriented from the horizontal meridian. On each trial, the bars were independently rotated from horizontal by about 10° (clockwise or anti-clockwise with equal probability), an angle predetermined using two alternate forced-choice procedures to yield approximately 85% correct performance for judging orientation. (Averaged across observers, performance for the bar-orientation judgment task was 85.0% correct for the right visual field and 86.8% correct for the left visual field.) The bar was randomly positioned within the 9° square to ensure that subject's attention was spread over the entire stimulus region. The square regions within which the bars could be positioned were displaced 1° from the principal meridians, the region on the right being identical to the location and size of the stimulus patch (see Fig. 1). The L-shaped attentional cue reverted back to a cross 500 ms after the offset of the stimuli. This was the signal for subjects to record their judgment of the orientation of the bar on the side to which they had attended. Following this judgment, for which no response deadline was imposed, the fixation cross remained for a further 1000 ms before the attentional cue was again presented. For each experimental condition, 100 trials were recorded for each ISI, and the resultant signals were band pass filtered at 1–100 Hz.

2.3. Recording

Magnetic responses were recorded using a 201-channel, whole-head biomagnetic imaging system (from Shimadzu, Kyoto, Japan). The responses were sampled at 500 Hz for 2048 ms, beginning 200 ms before the onset of the fixation cue indicating which direction to shift attention. Simultaneous recording of the electro-oculogram (EOG) was used to continually monitor eye movements. Artifact rejection was performed offline by removing epochs, with a peak amplitude exceeding 100 μV. Most trials (>95%) for each subject were <60 μV, and no systematic eye movement bias occurred for any subject.

2.4. Data analysis

ICA was conducted (using EEGLAB, [11]) over the normalized single-sweep data to separate sources in the magnetic signals that are spatially fixed and temporally independent [33,34] using a similar procedure as used in our previous studies [5,66]. In this analysis, the data from each experimental condition (attention directed towards or away from stimulus) were combined. The raw data for each single sweep of 201 channels was down-sampled from 500 Hz to 250 Hz and baseline normalized. Independent components (ICs) were determined using an unsupervised neural network to train a weight matrix that maximizes the joint entropy between the nonlinearly transformed channel data

[33]. Multiplying the original input data by the rows of the trained weight matrix gives the activation waveform for each IC. The columns of the inverse weight matrix show the relative sensor projection strengths of the respective components [33]. ICs were sorted in descending order of their mean projected variance.

In order to determine the IC of calcarine origin, all sensor projection maps (inverse weight matrix W^{-1}) were examined. The activation waveforms of the ICs showing large weights in sensor projection maps over occipital regions were projected onto the sensors by multiplication with the inverse weight matrix (W^{-1}) and were then subjected to a single-equivalent current dipole (ECD) analysis to determine the source location. Best-fit solutions were obtained using a least-squares error fit between the observed magnetic signals and those predicted by the ECD model. The solution yielding the best goodness of fit (GF) was determined as:

$$GF = 1 - \sqrt{\sum_{i=1}^{N} (S_i - D_i)^2 / \sum_{i=1}^{N} S_i^2} \qquad (1)$$

where N is a number of channels, S_i and D_i are the observed and predicted magnetic signals in channel i, respectively.

Event-related spectral perturbation (ERSP) plots [11] were generated for each condition and subject using the single-sweep activation waveforms of the calcarine components. The power spectrum was determined using a short-time Fourier transform, with a sliding latency window of 11.6 samples (46.7 ms) over the 425 samples ranging from −200 to 1500 ms postcue event onset sampled at 250 Hz. The sliding latency window was applied 32 times with a window size of 64 samples (256 ms) wide. The output of the ERSP therefore consisted of 32 sub-window centers ranging from −72 ms to 1372 ms. The results were oversampled two times, and the frequency range consisted of 25 equally spaced bins with central frequencies ranging from 1.95 Hz to 48.8 Hz. The 25 × 32 pixel (frequency × time) ERSP plots for each condition for each subject were saved as image files and used for random effects analysis (SPM2; Wellcome Department of Cognitive Neurology, University College, London). Multiple comparisons were corrected using the false discovery rate procedure (FDR) [19]. Significant spectral power increases and decreases were determined for each condition by a one-sample *t* test in which positive and negative deviations from zero (baseline) were assessed. Significant differences between the experimental conditions were assessed by a paired *t* test. We tested whether any observed power changes were phase-locked to the cue/stimulus onset (time locking events) by calculating the inter-trial coherence (ITC) [11,35] or phase locking factor [57].

2.5. Subjects

Fourteen subjects (aged 22–42 years) with no history of neurological injury were employed. All subjects gave written informed consent for the experimental procedures, which were approved by the ATR Human Subject Review Committee. All observers had normal or corrected-to-normal visual acuity and normal visual fields and color vision.

3. Results

All results reported in this section are for trials containing an ISI of 1000 ms unless otherwise stated.

3.1. Effects of attentional shift on global magnetic field power

The left-hand panels in Fig. 2 show the recorded MEG data for two subjects (NG and NY) plotted as global magnetic field power (GFP) over time. GFP was calculated as:

$$GFP(t) = \sqrt{\sum_{i=1}^{N} (S_i(t))^2 / N} \qquad (2)$$

where $S_i(t)$ is the observed magnetic signal in channel i at time t, and N is the number of channels. For each subject, GFP is plotted from 200 ms prior to the onset of the cue to shift attention to 500 ms poststimulus onset. The onset times of the attentional cue (0 ms) and stimulus (1000 ms) are demarcated by vertical dotted lines in each panel. Responses are shown for the condition whereby the observer's attention was directed either towards the expected stimulus (red functions) or away from it (blue functions). For each subject: (1) the red and blue functions remained virtually superimposed throughout the entire time period; (2) a weak sustained increase in GFP was evident during the postcue–prestimulus period; and (3) GFP peaked at approximately 120 ms poststimulus onset.

3.2. Spatial localization of neural current sources

For each subject, independent components (ICs) showing large weights in sensor projection maps over the occipital pole were found (based on the combined data sets for attention directed towards and away from the stimulus). ICs with sources localized to Brodmann's area 17 (calcarine cortex), as determined using dipolar analyses (see Materials and methods), were found in all subjects (see Table 1 for Talairach coordinates [55]).

The right-hand panels in Fig. 2 show the reconstructed power functions of the ICs representing calcarine activity. They are similar to the power functions calculated from the averaged MEG responses in two respects: (1) the attentional status of the observer had no discernable effect (the red and blue functions were virtually identical); and (2) the functions contained a major peak at around 120 ms poststimulus onset. Unlike the recorded data, however, no
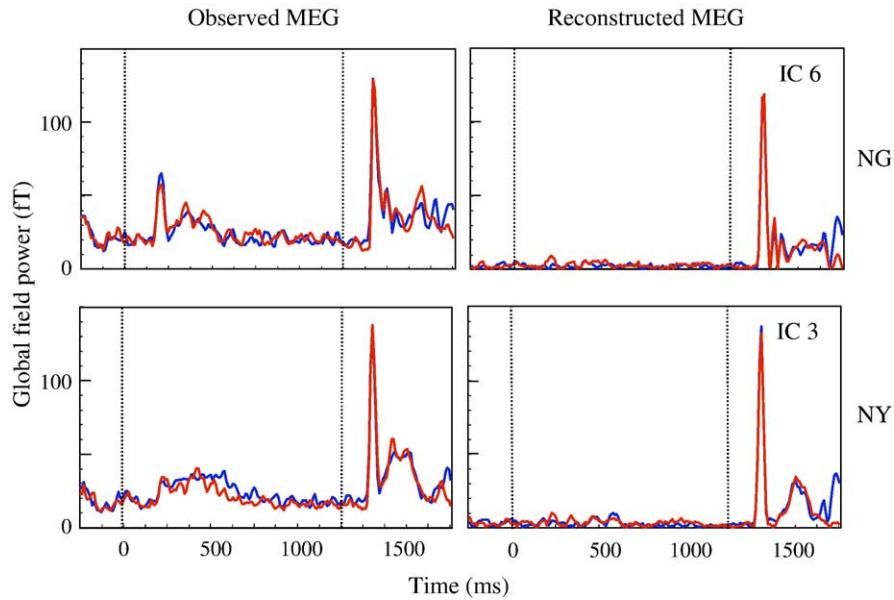
Fig. 2. Global magnetic field power (defined by Eq. (2)) plotted as a function of time for two subjects (NG and NY). The onset times of the attentional cue (0 ms) and stimulus (1000 ms) are demarcated by vertical dotted lines. GFP is shown for both experimental conditions: attention directed towards the stimulus (red line) and attention directed away from the stimulus (blue line). The left-hand panels show GFP for the observed MEG data. The right-hand panels show the reconstructed power functions of the independent components (ICs) representing activity in Brodmann's area 17. The IC number is shown in the upper right-hand corner of each panel.

increase in GFP was evident in the reconstructed power functions during the postcue–prestimulus period (compare left- and right-hand panels for each observer in Fig. 2).

Fig. 3 shows the dipole source solutions co-registered with sagittal and coronal MRI scans of subjects NG and NY. Note that for each subject the solution was adjacent to the calcarine sulcus in the left hemisphere (contralateral to the location of the expected stimulus). A dipolar analysis was also applied at a latency corresponding to the peak in the GFP plot of the recorded MEG data for each subject (Fig. 2, left-hand panels). As above, this analysis placed the

Table 1
List of the ICs with sources localized to Brodmann's area 17

Subject	IC number	Brain region	x	y	z	GF (%)
NG	IC 6	Occipital left cun BA 17	−1	−95	0	99
NY	IC 3	Occipital left cun BA 17	−2	−91	4	98
KSA	IC 6	Occipital left cun BA 17	−9	−87	9	99
AC	IC 9	Occipital left cun BA 17	−1	−92	4	97
NK	IC 3	Occipital left cun BA 17	−7	−91	5	97
SN	IC 13	Occipital left cun BA 17	−8	−94	4	93
MA	IC 12	Occipital left cun BA 17	−9	−92	3	94
US	IC 5	Occipital left cun BA 17	−4	−97	1	96
SY	IC 5	Occipital left cun BA 17	−1	−91	4	97
TY	IC 10	Occipital left cun BA 17	−2	−89	−4	98
RH	IC 6	Occipital left cun BA 17	−1	−98	−1	96
NS	IC 9	Occipital left cun BA 17	−10	−93	1	99
KSI	IC 7	Occipital left cun BA 17	−2	−89	1	99
IN	IC 6	Occipital left cun BA 17	−16	−84	8	98

The Talairach coordinates and brain regions [55] for the single equivalent current dipole of the ICs are shown for fourteen subjects. Abbreviations: cun, cuneus; BA, Brodmann's area; GF, goodness of fit. x, y and z are in mm.

underlying neural activity near the occipital pole, adjacent to the calcarine sulcus in the left hemisphere.

3.3. Effects of attentional shift on event-related spectral perturbation (ERSP) within the calcarine

For the ICs reflecting calcarine activity, group-mean ERSP plots [11] of the postcue spectral power differences (in decibels) referenced to a 200 ms precue baseline recording are shown in the top panels of Fig. 4(a, b). In each plot, the cue to shift attention appeared at $t = 0$ ms and the stimulus appeared at $t = 1000$ ms (shown as vertical dotted lines in each panel). Note that, when attention was directed either towards (Fig. 4b) or away from the expected stimulus (Fig. 4a), a decrease in spectral power (colored blue) was evident for frequencies near 10 Hz (alpha) throughout the last two thirds of the postcue–prestimulus period. Note also that, after stimulus onset (at 1000 ms), an increase in spectral power (colored red) was evident across a broad range of frequencies (approximately 2.0–49 Hz) under both experimental conditions (Figs. 4a, b).

The bottom panels in Fig. 4(c, d) show the results of a random effects one-sample t test indicating significant ($P < 0.05$ FDR corrected; $df = 13$) positive (power increases) and negative (power decreases) event-related spectral changes over the time course of each experimental condition. Fig. 4c shows the results for attention directed away from the stimulus and Fig. 4d towards the stimulus. Our analyses revealed that the observed spectral power decrease throughout the last two thirds of the postcue–prestimulus period was significantly deviated from baseline when attention was
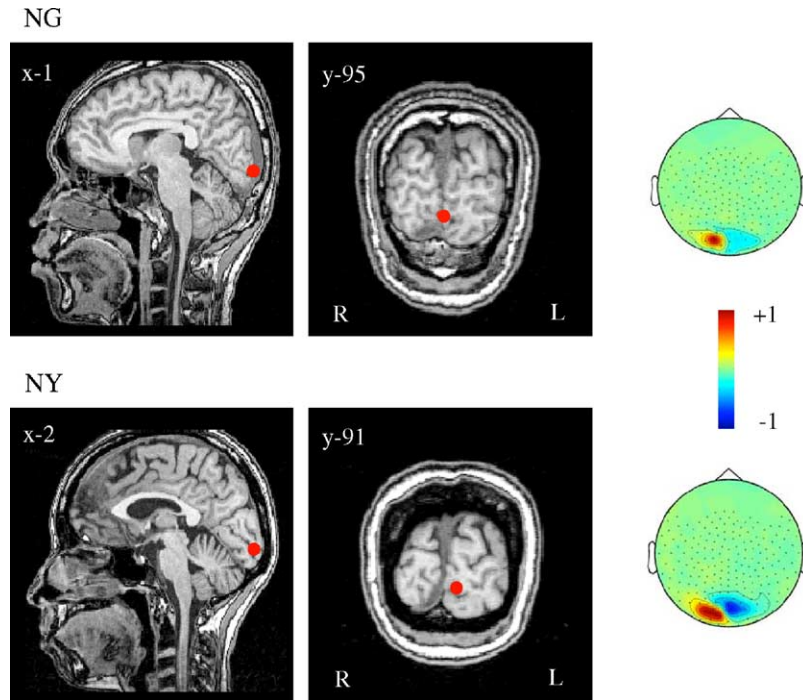
Fig. 3. Dipole source solutions (solid red circles) of the independent components (ICs) representing activity in Brodmann's area 17 (based on the combined data sets for attention directed towards and away from the stimulus), co-registered with sagittal and coronal MR images for subjects NG and NY. The Talairach coordinate for each solution is given in the upper left-hand corner of each plot. The sensor plane projection map W^{-1} for each subject is shown on the far right.
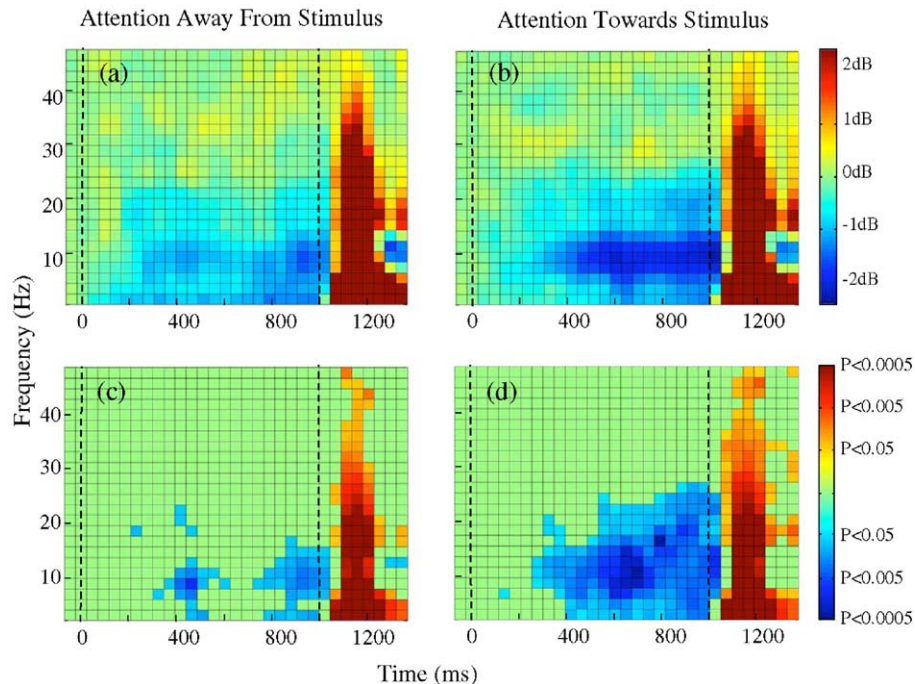

Fig. 4. Group analysis ($n = 14$) showing event-related spectral perturbation (ERSP) plots derived from the activation waveforms of the ICs reflecting calcarine activity for each subject and for each experimental condition (ISI = 1000 ms). The plots consist of 25 equally spaced bins with center frequencies ranging from 1.95 to 48.8 Hz and 32 equally spaced time steps with centers at −72 to 1372 ms. The group-mean ERSP plots show postcue power differences (in dB) referenced to a 200 ms precue baseline recording for (a) attention directed away from the stimulus and (b) attention directed towards the stimulus. Both spectral power increases (reddish hues) and decreases (bluish hues) are evident. A random effects one-sample t test indicating significant ($P < 0.05$ FDR corrected; $df = 13$) positive (reddish hues) and negative (bluish hues) event-related spectral power changes are shown for (c) attention directed away from the stimulus and (d) attention directed towards the stimulus. The cue onset time ($t = 0$ ms) and the stimulus onset time ($t = 1000$ ms) are indicated by vertical dotted lines in each plot.

directed towards stimulus (Fig. 4d). In contrast, when attention was directed away from the stimulus, the observed power decrease was only significant at or near 450 ms and 900 ms postcue onset (Fig. 4c). After stimulus onset, a significant spectral power increase across a broad range of frequencies was evident under both experimental conditions (Figs. 4c, d).

Fig. 5 shows a statistical significance map of the differences between the experimental conditions, as assessed using a random effects paired *t* test (*n* = 14). The region of interest (ROI) was set for frequencies from 7.8 Hz to 15.6 Hz (the area within the dotted lines), and multiple comparisons were corrected (*P* < 0.05, FDR corrected; *df* = 13). The ROI was selected a priori and based on physiological [15] and electrophysiological [13,16,65] evidence that attentional modulation may alter the amplitude of alpha-band (8–14 Hz) activity. Statistical evaluation of the different attentional conditions revealed significantly lower alpha activity when attention was directed towards the stimulus compared with attention directed away from it, beginning at about 600 ms postcue onset. In other words, evaluation of Fig. 4 indicates that the difference between conditions (Fig. 5) reflects a greater reduction in alpha activity when attention was directed towards the stimulus compared with attention away from it.

3.4. Inter-trial phase coherence within the calcarine

Fig. 6 shows the group-mean (*n* = 14) inter-trial coherence (ITC) [11,35] of the ICs representing calcarine activity in a frequency-by-latency image, showing the strength of phase locking across trials for two experimental conditions: (Fig. 6a) attention directed away from the stimulus and (Fig. 6b) attention directed towards the
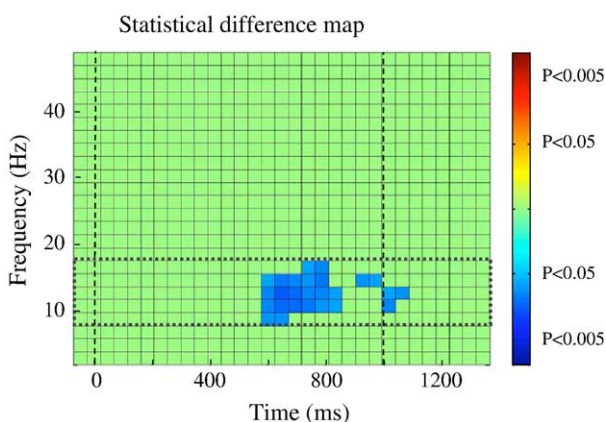

Fig. 5. Statistical significance map of the differences between the experimental conditions, as assessed using a random effects paired *t* test (*n* = 14). The region of interest (ROI) was set for the frequency range 7.8 Hz to 15.6 Hz (the area within the dotted lines), and multiple comparisons were corrected (*P* < 0.05, FDR corrected; *df* = 13). The blue areas indicate a significant decrease in spectral power when attention was directed towards the stimulus when compared with attention directed away from it. The onset times of the attentional cue (0 ms) and stimulus (1000 ms) are shown by vertical dotted lines.

stimulus. The onset times of the attentional cue (0 ms) and stimulus (1000 ms) are indicated by vertical dotted lines. The ITC measure varies from zero (non-phase-locked, blue-colored pixels) to 1 (phase-locked, red-colored pixels). Note that, for each experimental condition, ITC remained near zero for frequency ranges from 2 Hz to 49 Hz throughout the postcue–prestimulus period. This indicates that the postcue onset reduction in spectral power within the alpha-band frequency range (Fig. 4) must reflect induced (event-related desynchronization, ERD) activity [11,35]. After stimulus onset (at 1000 ms), ITC rose sharply and was near perfect for frequency ranges from 2 Hz to 25 Hz. This indicates that the poststimulus onset increase in spectral power across a broad range of frequencies (Fig. 4) must in large part reflect evoked (phase-locked) activity.

3.5. Effects of attentional shift on event-related spectral perturbation (ERSP) within the calcarine for the short ISI condition

Here, we report the analyses for the short (500 ms) ISI data, conducted using the same procedures as that described above for the long (1000 ms) ISI data. For each subject, independent components (ICs) with dipole sources adjacent to the calcarine sulcus in the left (contralateral) hemisphere were found. In general, the reconstructed magnetic field power functions of the ICs representing calcarine activity for the short ISI condition were similar to those for the long ISI condition. Namely, GFP (from Eq. (2)) peaked at about 120 ms after stimulus onset, there was no discernable difference between the field power functions based on the attentional status of the observer, and no increase in field power was evident during the postcue–prestimulus period.

Fig. 7(a, b) shows, for the ICs reflecting calcarine activity, group-mean ERSP plots for the short ISI condition, plotted in the same manner as those calculated for the long ISI condition (Figs. 4a, b). A decrease in spectral power was evident for frequencies near 10 Hz (alpha) when attention was directed towards the expected stimulus (Fig. 7b), beginning approximately 250 ms postcue onset and persisting until the onset of the stimulus at 500 ms. However, this reduction in spectral power was not statistically significant (Fig. 7d). Similarly, the weak reduction in spectral power evident during the postcue–prestimulus period when attention was directed away from the stimulus (Fig. 7a) was not statistically significant (Fig. 7c). After stimulus onset (at 500 ms), a significant (*P* < 0.05 FDR corrected; *df* = 13) spectral power increase across a broad range of frequencies was evident under both experimental conditions (Figs. 7c, d), as was the case for the long ISI condition (Figs. 4c, d).

4. Discussion

Our results provide evidence that shifts of attention to an expected visual target affect the amplitude of alpha-band
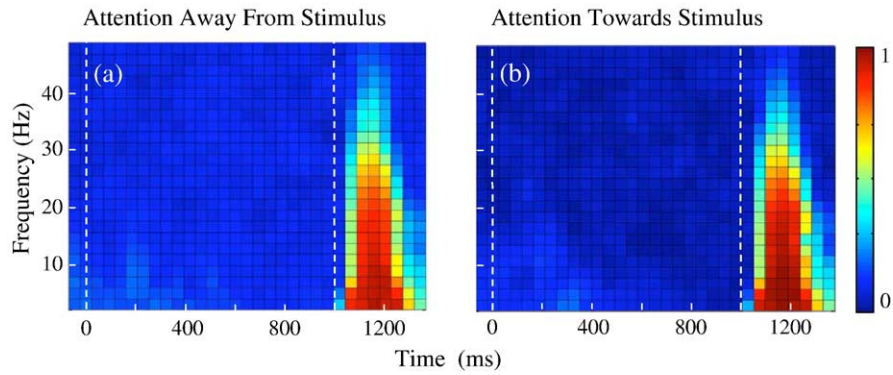
Fig. 6. Group-mean ($n = 14$) inter-trial coherence (ITC) [11,35] of the ICs representing calcarine activity, showing the strength of phase locking across trials for (a) attention directed away from the stimulus and (b) attention directed towards the stimulus. ITC varies from zero (non-phase-locked, blue-colored pixels) to 1 (phase-locked, red-colored pixels). The onset times of the cue (0 ms) and stimulus (1000 ms) are indicated by vertical dotted lines.

oscillatory activity in the human calcarine cortex (Figs. 4 and 5, long ISI condition). The amplitude changes examined were well-modeled with a single equivalent current dipole within Brodmann's area 17 contralateral to the location of the expected target (Fig. 3 and Table 1). This indicates that a significant proportion of the neuronal changes may originate from a focal source in early visual areas V1 and/or V2, although we cannot discount the fact that this source may reflect the center of gravity of a region that extends into

several early visual areas. We assume that the activity observed within the calcarine reflects the action of transient (attention shift) mechanisms of attentional control [30]. Together with the knowledge that higher-order visual areas are similarly affected by attentional shifts [7,29], our results lead us to suggest that attentional control processes may be fundamental to all stages of cortical visual processing.

The question remains as to whether the calcarine activity we observed reflects the primary source of an
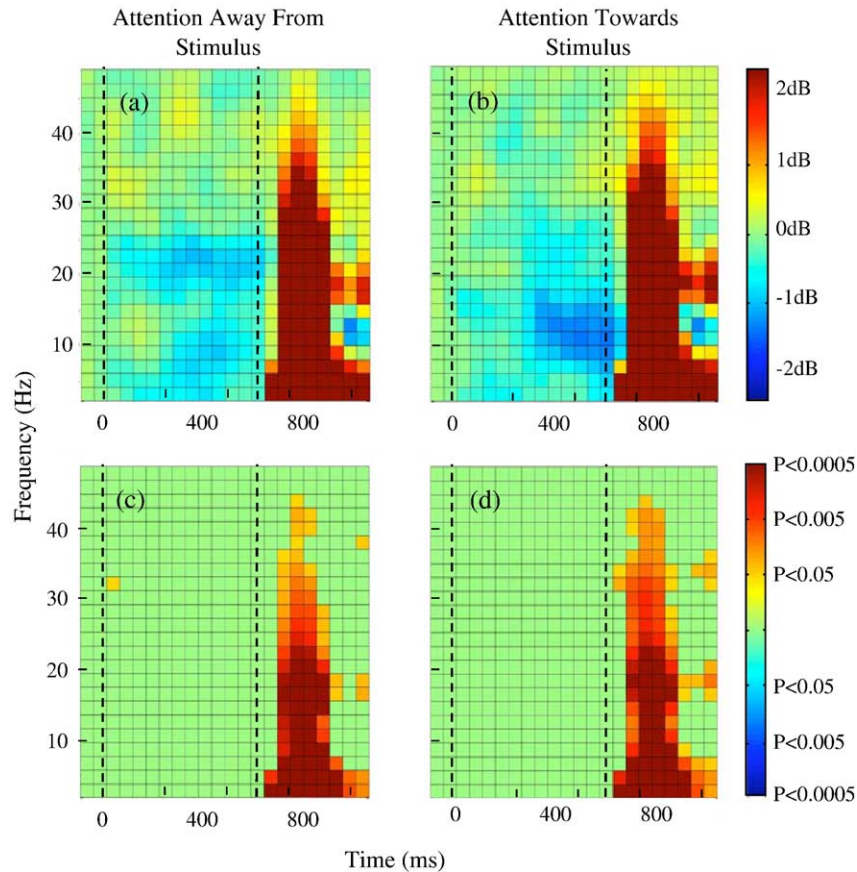

Fig. 7. Group analysis ($n = 14$) showing ERSP plots derived from the activation waveforms of the ICs reflecting calcarine activity for each subject and for each experimental condition for the short (500 ms) ISI condition. The plots consist of 25 equally spaced bins with center frequencies ranging from 1.95 to 48.8 Hz and 23 equally spaced time steps with centers at −72 to 872 ms. Other details are as reported in the legend to Fig. 4.

attentional control signal or whether it reflects a relay process forming part of an interareal communication network for attentional control. Many have argued that the fronto-parietal cortex is the primary source of top–down attentional control signals (reviewed in [9,28]). Indeed, it has been suggested that a common neural region located within the parietal cortex may subserve multiple modes of attentional control [64]. Nonetheless, our results provide clear evidence of cue-related (control of attention) activity in the calcarine prior to any stimulus-related activity. This is supported by Liu et al. [30] recent fMRI study showing that attentional shifts generate activity not only within the fronto-parietal cortex but also within the calcarine. However, Liu et al. argued that the observed calcarine activity was unlikely to represent the source of an attentional control signal because it is an early sensory area. They concluded that the calcarine activity probably reflects a 'refocusing' of attention. Assuming this to be the case, our results suggest a possible neural process by which an attentional refocusing (or relay) effect might be accomplished, namely, amplitude changes in alpha-band oscillatory activity.

A comparison of the different attentional conditions revealed amplitude changes in induced alpha-band oscillations within the calcarine throughout the last half of the postcue–prestimulus period (Fig. 5, long ISI condition). The results show a relative decrease in alpha activity when attention was directed towards the stimulus, beginning around 600 ms postcue onset and persisting until the appearance of the stimulus ($P < 0.05$, FDR corrected, $df = 13$). This is in general agreement with various electro-encephalographic (EEG) studies demonstrating that late components (500 ms–1000 ms after cue onset) in the postcue–prestimulus period are affected by the degree of stimulus expectancy and the attentional status of the observer [13,16,61,65]. Together with these studies, we speculate that the observed power decrease in alpha may be invariant with prestimulus delay period as no significant reductions in spectral power were evident during the postcue–prestimulus period for the short (500 ms) ISI condition (see Fig. 7). The functional significance of this late-onset decrease in alpha remains unclear, though presumably it reflects the neuronal operations associated with disengaging, shifting or engaging attention. There is evidence that only 50 ms to 120 ms may be needed for attention to shift from one locus to another [36,46], while the process of engaging attention may need substantially longer [36,58]. Together, these findings provide evidence that the late-onset decrease in alpha we observed may reflect a sustained attentional component which is responsible for engaging attention at a new spatial location.

There is clear evidence (Fig. 6) that the decrease in alpha activity we observed during the postcue–prestimulus period for the long ISI condition was induced (non-phase-locked), not evoked (i.e., phase-locked). Such a decrease in spectral power is often termed an event-related desynch-

ronization (ERD) [11,35]. That there was no evoked activity during this time period explains why the attentional status of the observer had no discernable effect on averaged global field power (see Fig. 2). Assuming that induced activity reflects changes in the coordinated activity of cortical neurons [32,41], our MEG data provide evidence to suggest that attentional shifts to an expected visual target alter the strength of interactions between neurons in the calcarine.

The relative decrease in alpha (ERD) shown in Fig. 5 is consistent with multi-unit recordings in monkey [15] and EEG recordings in human [13,16,65] showing reductions in low frequency (<17 Hz) activity with attentional shifts. The origin of alpha rhythms and their role in information processing both within and between brain areas continue to be debated. There is evidence that both thalamo-cortical and cortico-cortico neurons play an important role in the generation of alpha-band rhythms [31,54], and it has been reported that a desynchronized EEG in alpha represents an activated level of those neurons [54]. Therefore, it has been proposed that ERD in alpha can be interpreted as an electrophysiological correlate of activated cortical areas involved in sensory and/or cognitive processing [40,41]. An observed desynchronization in the EEG (or MEG) indicates that, in the corresponding brain areas, neurons are working relatively independently [40] and as such may have a high capacity for carrying information [45]. Based on the concepts of information theory [48], Thatcher and colleagues [59] have argued similarly that, when the underlying generators of the observed EEG are highly coherent (synchronized) with one another, they have less capacity for coding either external signals or internal signals from other groups of neurons. Accepting these arguments from information theory, we speculate that the reduction in alpha activity we observe following a shift of attention may serve to place the sensory cortex in a heightened state of readiness for coding incoming information. We conclude that attentional processes act as a priming mechanism to enhance neuronal processing by rendering the calcarine cortex active prior to visual input.

Our results may also be consistent with several fMRI studies which show that a shift or modulation of attention leads to a relative increase in the hemodynamic baseline signal [7,26,29]. This is so because an increase in the hemodynamic signal may be the signature for a localized decrease in low frequency oscillatory activity [50]. Using the same experimental paradigm to assess visual motion processing with both MEG and fMRI, Singh et al. [50] showed that the location of the hemodynamic signal was often remarkably similar to that of frequency-specific decreases in cortical power within the alpha and beta bands (as identified with MEG beamformer analyses). Thus, the sustained postcue decrease in alpha reported here may form the neural basis of the attentional effects reported in fMRI studies.

Acknowledgments

References

[1] S.J. Anderson, Functional neuroimaging in amblyopia, in: M. Mosely, A. Fielder (Eds.), Amblyopia: A Multidisciplinary Approach, Butterworth Heinemann, Oxford, 2002, pp. 43–67.

[2] S.J. Anderson, I.E. Holliday, G.F. Harding, Assessment of cortical dysfunction in human strabismic amblyopia using magnetoencephalography (MEG), Vision Res. 39 (1999) 1723–1738.

[3] E. Basar, M. Schurmann, C. Basar-Eroglu, S. Karakas, Alpha oscillations in brain functioning: an integrative theory, Int. J. Psychophysiol. 26 (1997) 5–29.

[4] E. Basar, C. Basar-Eroglu, S. Karakas, M. Schurmann, Gamma, alpha, delta, and theta oscillations govern cognitive processes, Int. J. Psychophysiol. 39 (2001) 241–248.

[5] D.E. Callan, A.M. Callan, C. Kroos, E. Vatikiotis-Bateson, Multimodal contribution to speech perception revealed by independent component analysis: a single-sweep EEG case study, Brain Res. Cogn. Brain Res. 10 (2001) 349–353.

[6] M. Chatila, C. Milleret, P. Buser, A. Rougeul, A 10 Hz "alpha-like" rhythm in the visual cortex of the waking cat, Electroencephalogr. Clin. Neurophysiol. 83 (1992) 217–222.

[7] D. Chawla, G. Rees, K.J. Friston, The physiological basis of attentional modulation in extrastriate visual areas, Nat. Neurosci. 2 (1999) 671–676.

[8] C. Constantinidis, M.A. Steinmetz, Neuronal responses in area 7a to multiple-stimulus displays: I. Neurons encode the location of the salient stimulus, Cereb. Cortex 11 (2001) 581–591.

[9] M. Corbetta, G.L. Shulman, Control of goal-directed and stimulus-driven attention in the brain, Nat. Rev., Neurosci. 3 (2002) 201–215.

[10] M. Corbetta, J.M. Kincade, J.M. Ollinger, M.P. McAvoy, G.L. Shulman, Voluntary orienting is dissociated from target detection in human posterior parietal cortex, Nat. Neurosci. 3 (2000) 292–297.

[11] A. Delorme, S. Makeig, EEGLAB: an open source toolbox for analysis of single-trial EEG dynamics including independent component analysis, J. Neurosci. Methods 134 (2004) 9–21.

[12] S. Engel, X. Zhang, B. Wandell, Colour tuning in human visual cortex measured with functional magnetic resonance imaging, Nature 388 (1997) 68–71.

[13] J.J. Foxe, G.V. Simpson, S.P. Ahlfors, Parieto-occipital approximately 10 Hz activity reflects anticipatory state of visual attention mechanisms, NeuroReport 9 (1998) 3929–3933.

[14] S.R. Friedman-Hill, L.C. Robertson, R. Desimone, L.G. Ungerleider, Posterior parietal cortex and the filtering of distractors, Proc. Natl. Acad. Sci. U. S. A. 100 (2003) 4263–4268.

[15] P. Fries, J.H. Reynolds, A.E. Rorie, R. Desimone, Modulation of oscillatory neuronal synchronization by selective visual attention, Science 291 (2001) 1560–1563.

[16] K.M. Fu, J.J. Foxe, M.M. Murray, B.A. Higgins, D.C. Javitt, C.E. Schroeder, Attention-dependent suppression of distracter visual input can be cross-modally cued as indexed by anticipatory parieto-occipital alpha-band oscillations, Brain Res. Cogn. Brain Res. 12 (2001) 145–152.

[17] F. Fylan, I.E. Holliday, K.D. Singh, S.J. Anderson, G.F. Harding, Magnetoencephalographic investigation of human cortical area V1 using color stimuli, NeuroImage 6 (1997) 47–57.

[18] S.P. Gandhi, D.J. Heeger, G.M. Boynton, Spatial attention affects brain activity in human primary visual cortex, Proc. Natl. Acad. Sci. U. S. A. 96 (1999) 3314–3319.

[19] C.R. Genovese, N.A. Lazar, T. Nichols, Thresholding of statistical maps in functional neuroimaging using the false discovery rate, NeuroImage 15 (2002) 870–878.

[20] B. Giesbrecht, M.G. Woldorff, A.W. Song, G.R. Mangun, Neural mechanisms of top–down control during spatial and feature attention, NeuroImage 19 (2003) 496–512.

[21] J. Gottlieb, Parietal mechanisms of target representation, Curr. Opin. Neurobiol. 12 (2002) 134–140.

[22] J.P. Gottlieb, M. Kusunoki, M.E. Goldberg, The representation of visual salience in monkey parietal cortex, Nature 391 (1998) 481–484.

[23] M.R. Harter, S.L. Miller, N.J. Price, M.E. LaLonde, A.L. Keyes, Neural processes involved in directing attention, J. Cogn. Neurosci. 1 (1989) 223–237.

[24] H.L. Hawkins, S.A. Hillyard, S.J. Luck, M. Mouloua, C.J. Downing, D.P. Woodward, Visual attention modulates signal detectability, J. Exp. Psychol. Hum. Percept. Perform. 16 (1990) 802–811.

[25] A. Hillebrand, G.R. Barnes, A quantitative assessment of the sensitivity of whole-head MEG to activity in the adult human cortex, NeuroImage 16 (2002) 638–650.

[26] J.B. Hopfinger, M.H. Buonocore, G.R. Mangun, The neural mechanisms of top–down attentional control, Nat. Neurosci. 3 (2000) 284–291.

[27] D.A. Jeffreys, J.G. Axford, Source locations of pattern-specific components of human visual evoked potentials. I. Component of striate cortical origin, Exp. Brain Res. 16 (1972) 1–21.

[28] S. Kastner, L.G. Ungerleider, Mechanisms of visual attention in the human cortex, Annu. Rev. Neurosci. 23 (2000) 315–341.

[29] S. Kastner, M.A. Pinsk, P. De Weerd, R. Desimone, L.G. Ungerleider, Increased activity in human visual cortex during directed attention in the absence of visual stimulation, Neuron 22 (1999) 751–761.

[30] T. Liu, S.D. Slotnick, J.T. Serences, S. Yantis, Cortical mechanisms of feature-based attentional control, Cereb. Cortex 13 (2003) 1334–1343.

[31] F. Lopes da Silva, Neural mechanisms underlying brain waves: from neural membranes to networks, Electroencephalogr. Clin. Neurophysiol. 79 (1991) 81–93.

[32] F.H. Lopes da Silva, G. Pfurtscheller, Basic concepts on EEG synchronization and desynchronization, in: G. Pfurtscheller, F.H. Lopes da Silva (Eds.), Event-related Desynchronization, Revised SeriesHandb. Electroencephalogr. Clin. Neurophysiol., vol. 6, Elsevier B.V., 1999, pp. 3–11.

[33] S. Makeig, T.P. Jung, A.J. Bell, D. Ghahremani, T.J. Sejnowski, Blind separation of auditory event-related brain responses into independent components, Proc. Natl. Acad. Sci. U. S. A. 94 (1997) 10979–10984.

[34] S. Makeig, C. Humphries, T.P. Jung, T. Bell, M. McKeown, A. Dimitrov, T.W. Lee, J.F. Cardoso, MATLAB Functions for Psychophysiological Data Analysis, CNL/Salk Institute, 2001.

[35] S. Makeig, S. Debener, J. Onton, A. Delorme, Mining event-related brain dynamics, Trends Cogn. Sci. 8 (2004) 204–210.

[36] K. Nakayama, M. Mackeben, Sustained and transient components of focal visual attention, Vision Res. 29 (1989) 1631–1647.

[37] A.C. Nobre, G.N. Sebestyen, C. Miniussi, The dynamics of shifting visuospatial attention revealed by event-related potentials, Neuropsychologia 38 (2000) 964–974.

[38] P.L. Nunez, B.M. Wingeier, R.B. Silberstein, Spatial–temporal structures of human alpha rhythms: theory, microcurrent sources, multiscale measurements, and global binding of local networks, Hum. Brain Mapp. 13 (2001) 125–164.

[39] H. Pashler, The Psychology of Attention, MIT Press, Cambridge, MA, 1999.

[40] G. Pfurtscheller, Functional brain imaging based on ERD/ERS, Vision Res. 41 (2001) 1257–1260.

[41] G. Pfurtscheller, F.H. Lopes da Silva, Event-related EEG/MEG synchronization and desynchronization: basic principles, Clin. Neurophysiol. 110 (1999) 1842–1857.

[42] M.I. Posner, S.E. Petersen, The attention system of the human brain, Annu. Rev. Neurosci. 13 (1990) 25–42.

[43] M.I. Posner, J.A. Walker, F.J. Friedrich, R.D. Rafal, Effects of parietal injury on covert orienting of attention, J. Neurosci. 4 (1984) 1863–1874.

[44] D. Ress, B.T. Backus, D.J. Heeger, Activity in primary visual cortex predicts performance in a visual detection task, Nat. Neurosci. 3 (2000) 940–945.

[45] F. Rieke, D. Warland, R.R. van Steveninck, W. Bialek, SPIKES: Exploring the Neural Code, MIT Press, Cambridge, MA, 1997.

[46] D. Sagi, B. Julesz, "Where" and "what" in vision, Science 228 (1985) 1217–1219.

[47] M. Schurmann, E. Basar, Functional aspects of alpha oscillations in the EEG, Int. J. Psychophysiol. 39 (2001) 151–158.

[48] C.E. Shannon, A mathematical theory of communication, Bell System Technical Journal, 27 (1948) 379–423, 623–656.

[49] J.C. Shaw, The Brain's Alpha Rhythms and the Mind, Elsevier Science Ltd., Amsterdam, The Netherlands, 2003.

[50] K.D. Singh, G.R. Barnes, A. Hillebrand, E.M. Forde, A.L. Williams, Task-related changes in cortical synchronization are spatially coincident with the hemodynamic response, NeuroImage 16 (2002) 103–114.

[51] S.D. Slotnick, J. Schwarzbach, S. Yantis, Attentional inhibition of visual processing in human striate and extrastriate cortex, NeuroImage 19 (2003) 1602–1611.

[52] A.T. Smith, K.D. Singh, M.W. Greenlee, Attentional suppression of activity in the human visual cortex, NeuroReport 11 (2000) 271–277.

[53] D.C. Somers, A.M. Dale, A.E. Seiffert, R.B. Tootell, Functional MRI reveals spatially specific attentional modulation in human primary visual cortex, Proc. Natl. Acad. Sci. U. S. A. 96 (1999) 1663–1668.

[54] M. Steriade, P. Gloor, R.R. Llinas, F.H. Lopes de Silva, M.M. Mesulam, Report of IFCN committee on basic mechanisms. Basic mechanisms of cerebral rhythmic activities, Electroencephalogr. Clin. Neurophysiol. 76 (1990) 481–508.

[55] J. Talairach, P. Tournoux, Co-Planar Stereotaxic Atlas of the Human Brain: 3-Dimensional Proportional System: An Approach to Cerebral Imaging, Thieme Medical Publishers, Inc., New York, 1988.

[56] C. Tallon-Baudry, Oscillatory synchrony and human visual cognition, J. Physiol. (Paris) 97 (2003) 355–363.

[57] C. Tallon-Baudry, O. Bertrand, C. Delpuech, J. Pernier, Stimulus specificity of phase-locked and non-phase-locked 40 Hz visual responses in human, J. Neurosci. 16 (1996) 4240–4249.

[58] Y. Tanaka, S. Shimojo, Temporal and spatial characteristics of attention to facilitate manual and eye-movement responses, Perception 30 (2001) 283–302.

[59] R.W. Thatcher, R. McAlaster, M.L. Lester, R.L. Horst, D.S. Cantor, Hemispheric EEG asymmetries related to cognitive functioning in children, in: A. Perecuman (Ed.), Cognitive Processing in the Right Hemisphere, Academic Press, New York, 1983, pp. 125–145.

[60] R.B. Tootell, N. Hadjikhani, E.K. Hall, S. Marrett, W. Vanduffel, J.T. Vaughan, A.M. Dale, The retinotopy of visual spatial attention, Neuron 21 (1998) 1409–1422.

[61] J. van Velzen, M. Eimer, Early posterior ERP components do not reflect the control of attentional shifts toward expected peripheral events, Psychophysiology 40 (2003) 827–831.

[62] A. von Stein, C. Chiang, P. Konig, Top–down processing mediated by interareal synchronization, Proc. Natl. Acad. Sci. U. S. A. 97 (2000) 14748–14753.

[63] T. Watanabe, Y. Sasaki, S. Miyauchi, B. Putz, N. Fujimaki, M. Nielsen, R. Takino, S. Miyakawa, Attention-regulated activity in human primary visual cortex, J. Neurophysiol. 79 (1998) 2218–2221.

[64] E. Wojciulik, N. Kanwisher, The generality of parietal involvement in visual attention, Neuron 23 (1999) 747–764.

[65] M.S. Worden, J.J. Foxe, N. Wang, G.V. Simpson, Anticipatory biasing of visuospatial attention indexed by retinotopically specific alpha-band electroencephalography increases over occipital cortex, J. Neurosci. 20 (2000) RC63.

[66] N. Yamagishi, D.E. Callan, N. Goda, S.J. Anderson, Y. Yoshida, M. Kawato, Attentional modulation of oscillatory activity in human visual cortex, NeuroImage 20 (2003) 98–113.

[67] S. Yamaguchi, H. Tsuchiya, S. Kobayashi, Electroencephalographic activity associated with shifts of visuospatial attention, Brain 117 (Pt. 3) (1994) 553–562.

[68] S. Yamaguchi, H. Tsuchiya, S. Kobayashi, Electrophysiologic correlates of visuo-spatial attention shift, Electroencephalogr. Clin. Neurophysiol. 94 (1995) 450–461.